bioRxiv preprint doi: https://doi.org/10.1101/2022.08.17.503990; this version posted August 18, 2022. The copyright holder for this preprint (which was not certified by peer review) is the author/funder. All rights reserved. No reuse allowed without permission.

Single molecule long-read real-time amplicon-based sequencing of *CYP2D6*: a proof-of-concept with hybrid haplotypes

Rachael Dong[1*] BSc, Megana Thamilselvan[2*], Xiuying Hu[3] MSc, Beatriz Carvalho Henriques[3] MSc, Yabing Wang[3] PhD, Keanna Wallace[3] BSc, Sudhakar Sivapalan[3] MSc, Avery Buchner[1,3] BSc, Vasyl Yavorskyy[2, 3] BSc, Kristina Martens[4] BSc, Wolfgang Maier[5] MD, Neven Henigsberg[6] PhD, Joanna Hauser[7] PhD, Annamaria Cattaneo[8, 9] PhD, Ole Mors[10] PhD, Marcella Rietschel[11] MD, Gerald Pfeffer[4,12] PhD, Katherine J. Aitchison[1,3,13, 14, 15, 16**] PhD

[1]University of Alberta, Neuroscience and Mental Health Institute, University of Alberta, Edmonton, Canada
[2]University of Alberta, College of Natural and Applied Sciences, Faculty of Science, Department of Biological Sciences, Edmonton, Canada
[3]University of Alberta, College of Health Sciences, Department of Psychiatry, Edmonton, Canada
[4]University of Calgary, Cumming School of Medicine, Hotchkiss Brain Institute, Department of Clinical Neurosciences, University of Calgary, Calgary, Canada
[5]University of Bonn, Department of Psychiatry and Psychotherapy, Bonn, Germany
[6]University of Zagreb School of Medicine, Centre for Excellence for Basic, Clinical and Translational Research, Croatian Institute for Brain Research, Zagreb, Croatia
[7]Poznan University of Medical Sciences, Department of Psychiatry, Poznan, Poland
[8]IRCCS Istituto Centro San Giovanni di Dio Fatebenefratelli, Biological Psychiatry Unit, Brescia, Italy.
[9]University of Milan, Department of Pharmacological and Biomolecular Sciences, Milan, Italy.
[10]Aarhus University Hospital, Psychosis Research Unit, Risskov, Denmark
[11]Heidelberg University, Medical Faculty of Mannheim, Central Institute of Mental Health, Department of Genetic Epidemiology in Psychiatry, Mannheim, Germany
[12]University of Calgary, Cumming School of Medicine, Alberta Child Health Research Institute & Department of Medical Genetics, Calgary, Canada
[13]University of Alberta, College of Health Sciences, Department of Medical Genetics, Edmonton, Canada
[14]King's College London, Institute of Psychiatry, Psychology and Neuroscience, Social, Genetic and Developmental Psychiatry Centre, London, England
[15]Northern Ontario School of Medicine, Thunder Bay, Canada
[16]University of Alberta, Women and Children's Research Institute, Edmonton, AB Canada

*These authors contributed equally to this work

**Corresponding author:

Dr. Katherine J. Aitchison, Neuroscience and Mental Health Institute; Women and Children's Research Institute; College of Health Sciences, Faculty of Medicine and Dentistry, Departments of Psychiatry and Medical Genetics, University of Alberta, Edmonton, AB T6G 2E1, Canada

Telephone: 1-780-492-4018; Email: kaitchis@ualberta.ca

Running Title: ***SMRT multiplexed amplicon sequencing of CYP2D6***

bioRxiv preprint doi: https://doi.org/10.1101/2022.08.17.503990; this version posted August 18, 2022. The copyright holder for this preprint (which was not certified by peer review) is the author/funder. All rights reserved. No reuse allowed without permission.

Abstract

CYP2D6 is a widely expressed human xenobiotic metabolizing enzyme, best known for its role in the hepatic phase I metabolism of up to 25% of prescribed medications, which is also expressed in other organs including the brain, where its potential role in physiology and mental health traits and disorders is under further investigation. Owing to the presence of homologous pseudogenes in the *CYP2D* locus and transposable repeat elements in the intergenic regions, the gene encoding the CYP2D6 enzyme, *CYP2D6*, is one of the most hypervariable known human genes - with more than 140 core haplotypes. Haplotypes include structural variants, with a subtype of these known as fusion genes comprising part of *CYP2D6* and part of its adjacent pseudogene, *CYP2D7*. The fusion genes are particularly challenging to identify. The CYP2D6 enzyme activity corresponding to some of these fusion genes is known, while for others it is unknown. The most recent (high fidelity, or HiFi) version of single molecule real-time (SMRT) long-read sequencing can cover whole *CYP2D6* haplotypes in a single continuous sequence read, ideal for structural variant detection. In addition, the accuracy of base calling has increased to a level sufficient for accurate characterization of single nucleotide variants. As new *CYP2D6* haplotypes are continuously being discovered, and likely many more remain to be identified in populations that are relatively understudied to date, a method of characterization that employs sequencing with at least this degree of accuracy is required. The aim of the work reported herein was to develop an efficient and accurate HiFi SMRT amplicon-based method capable of detecting the full range of *CYP2D6* haplotypes including fusion genes. We report proof-of-concept for 20 amplicons, aligned to fusion gene haplotypes, with prior cross-validation data. Amplicons with *CYP2D6-D7* fusion genes aligned to **36*, **63*, **68*, and **4* (**4-like*; **4N*, or **4.013*) hybrid haplotypes. Amplicons with *CYP2D7-D6* fusion genes aligned to the **13* subhaplotypes predicted (e.g., **13F*, **13A2*). Data analysis was efficient, and further method development indicates that this technique could suffice for the characterization of the full range of *CYP2D6* haplotypes. Although included in drug labelling by regulatory bodies (the U.S. Food and Drug Administration, the European Medicines Agency, the Pharmaceuticals and Medical Devices Agency) and prescribing recommendations by consortia (Clinical Pharmacogenetics Implementation Consortium and the Dutch Pharmacogenetics Working Group), the identification of *CYP2D6* variants is not yet routine in clinical practice. The HiFi sequencing method reported herein is suitable for high throughput, efficient, identification of the full range of known *CYP2D6* haplotypes and novel haplotypes, and

bioRxiv preprint doi: https://doi.org/10.1101/2022.08.17.503990; this version posted August 18, 2022. The copyright holder for this preprint (which was not certified by peer review) is the author/funder. All rights reserved. No reuse allowed without permission.

can be completed in a week or less. Moreover, the method that we have developed could be extended to other complex loci and to other species in a multiplexed high throughput assay.

bioRxiv preprint doi: https://doi.org/10.1101/2022.08.17.503990; this version posted August 18, 2022. The copyright holder for this preprint (which was not certified by peer review) is the author/funder. All rights reserved. No reuse allowed without permission.

Introduction

CYP2D6 is a xenobiotic metabolizing enzyme widely expressed in multiple organs including the liver, intestine, brain, gonads, and thyroid gland (Miksys et al., 2005; Aitchison et al., 2010; GTEx Portal, 2021). While it is best known for its role in hepatic phase I drug metabolism, where it plays a key role in the metabolism of an estimated 20-25% of all clinically used drugs (Ingelman-Sundberg, 2005; Zanger et al., 2013), it also has physiological roles. In the brain, it is found in cerebellar Purkinje cells and cortical pyramidal neurones (GTEx, 2021; Siegle et al., 2001). It is colocalized with the dopamine transporter (Niznik et al., 1990), and dopamine transporter inhibitors such as cocaine also inhibit CYP2D6 (Shen et al., 2007; Han et al., 2006). Enzyme activity appears to modulate resting brain perfusion, with suggestive involvement in regions associated with alertness or serotonergic function (Kirchheiner et al., 2011), and a rodent model developed to further explore this (Cheng et al., 2013). It is involved in steroid biosynthesis (conducting the 21-hydroxylation of progesterone and allopregnanolone; Niwa et al., 2008), as well as in the synthesis of dopamine from *m*- and *p*-tyramine (Hiroi et al., 1998; Funae et al., 2003), and of serotonin from 5-methoxyndolethylamines (Yu et al., 2003) including 5-methoxytryptamine (a metabolite and precursor of melatonin; Yu et al., 2003). The enzyme is induced in alcoholism (Miksys et al., 2002) and also in pregnancy (Pan et al., 2017). There has also been suggestive evidence of an association between enzyme status and personality traits (Bertilsson et al., 1989; Gan et al., 2004; Gonzalez et al., 2008).

The gene encoding the CYP2D6 enzyme, *CYP2D6*, lies at chromosome 22q13.2 adjacent to two pseudogenes, *CYP2D7* and *CYP2D8*. The three genes are highly homologous (Kimura et al., 1989; Yasukochi and Satta, 2011; Yang et al., 2017), and this, together with transposable repeat elements in the intergenic regions (Yasukochi and Satta, 2011), predisposes the locus to the generation of structural variants and novel mutations. Indeed, with more than 140 core haplotypes (or strings of genetic variants) identified to date (PharmVar, 2022a; Gaedigk et al., 2018), *CYP2D6* is one of the most hypervariable known human genes. Variants include single nucleotide variants (SNVs), small insertions and/or deletions (indels), and structural variants (PharmVar, 2022b). Structural variants include gene duplications and multiplications, complete deletions of the entire gene, and recombination events involving *CYP2D7* (Kramer et al., 2009 Gaedigk et al., 2010b; Black et al., 2012; Gaedigk, 2013; PharmVar, 2022b). The recombination events involving *CYP2D7* result in the formation of hybrid or fusion genes (Figure 1; Panserat et al., 1995; Daly et

bioRxiv preprint doi: https://doi.org/10.1101/2022.08.17.503990; this version posted August 18, 2022. The copyright holder for this preprint (which was not certified by peer review) is the author/funder. All rights reserved. No reuse allowed without permission.

al., 1996; Kramer et al., 2009; Gaedigk et al., 2008; 2010a, 2010b, 2014; Black et al., 2012; PharmVar, 2022b). *CYP2D7-2D6* fusions have a 5'-portion derived from *CYP2D7* and a 3'-portion derived from *CYP2D6*; these hybrids are non-functional (PharmVar, 2022b). *CYP2D6-2D7* fusions have a 5'-portion derived from *CYP2D6* and a 3'-portion derived from *CYP2D7*.

The Pharmacogene Variation Consortium assigns levels of function (no function, decreased, normal, or increased) to *CYP2D6* haplotypes that correspond to enzyme or phenotype predictions (poor metabolizers, intermediate, normal, or ultrarapid, respectively) (PharmVar, 2022a; Caudle et al., 2020). There have been recent refinements to the decreased function category (Caudle et al., 2020; Jukić et al., 2021; van der Lee et al., 2021). As an example of haplotype to phenotype prediction, an individual with two no function (or null) haplotypes is a poor metabolizer, with no active enzyme. This has implications for the metabolism of relevant medications. In this example, such individuals are unable to metabolize codeine from its inactive prodrug status to the metabolite with analgesic effect and hence do not experience any analgesic effect with this medication (Crews et al., 2021). The hybrid haplotypes have zero function, reduced function, or uncertain/unknown function (PharmVar, 2022a, 2022b). Hybrid haplotypes are found either as a single haplotype or in tandem with another *CYP2D6* haplotype (Kramer et al., 2009; Black et al., 2012; Gaedigk et al., 2010a, 2010b, 2014; PharmVar, 2022b).

CYP2D6 hybrid haplotypes are common in the general population, with a frequency estimated as at least 6.7% (Dalton et al., 2020). In our sample of 853 patients with depression, the frequency is 2.6% (22/853). Owing to the range of enzyme phenotype corresponding to *CYP2D6* hybrids, their accurate detection is important for predicting prescribing implications (Dalton et al., 2020), as well as potentially for neuroscience and physiology more generally.

The detection of *CYP2D6* hybrid haplotypes is however, challenging for many genomic technologies, with incorrect and incomplete characterization (Carvalho Henriques et al., 2021b). For example, the AmpliChip CYP450 Test did not cover hybrid haplotypes, and hence none of the 19 patients subsequently identified as having hybrid haplotypes had previously had these found, with 2 having been genotyped as *CYP2D6*1/*1* (wild-type) and 4 as 'no call.' (Carvalho Henriques et al., 2021b). We have previously reported the use of methods including Sanger sequencing to characterize hybrid haplotypes (Carvalho Henriques et al., 2020a, 2021a, 2021b). However, Sanger sequencing poses limitations for haplotype phasing (determining which combination of variants lies on which allele) and discriminating whether sequence is derived from

bioRxiv preprint doi: https://doi.org/10.1101/2022.08.17.503990; this version posted August 18, 2022. The copyright holder for this preprint (which was not certified by peer review) is the author/funder. All rights reserved. No reuse allowed without permission.

CYP2D6 or *CYP2D7* (Ardui et al., 2018). As a relatively labour-intensive and time-consuming technique, Sanger sequencing is best suited to low throughput.

Short-read next generation sequencing (NGS) is useful for the detection of SNVs and small indels, but less useful for structural variant detection with haplotype phasing, which require information across longer sequence or read lengths (Wenger et al., 2019). Single molecule real-time (SMRT) long-read sequencing provided by Pacific Biosciences (PacBio) and Oxford Nanopore (ONT) can achieve structural variant detection with haplotype phasing. However, until relatively recently, these SMRT technologies had a lower accuracy than short-read NGS. In 2019, circular consensus sequencing (CCS) was optimized to generate highly accurate (99.8%) long high fidelity (HiFi) reads (Wenger et al., 2019), with a median length of 13.4 kb (van der Lee et al., 2022). At this accuracy level, SNVs and short indels may be identified as well as structural variants. With *CYP2D6* haplotypes being under 10 kb and including all types of variation, this technology is eminently suited for the identification of the full range of haplotypes including novel, unidentified haplotypes. The latter is important as to date, there are populations (e.g., Indigenous peoples) in which this gene is relatively less studied than in others.

Some *CYP2D6* sequencing using HiFi SMRT has already been conducted. For 25 individuals with prior AmpliChip CYP450 genotype, including four with "*XN*" representing more than one copy of specific haplotypes (e.g., *CYP2D6*1/*2XN*), all genotypes were concordant with the genotype resulting from the SMRT data other than one (Buermans et al., 2017). In this case, the prior genotype was *CYP2D6*4/*4* and the new genotype was *CYP2D6*4/*5*, with the *CYP2D6*5* representing a complete deletion of the *CYP2D6* gene that had been missed by the AmpliChip (the design of which is now recognized as being able to detect only a subset of *CYP2D6*5* haplotypes; Carvalho Henriques et al., 2021b). In addition, one novel trinucleotide deletion and one novel SNV were detected in this group of samples, and confirmed by Sanger sequencing. SMRT data for *CYP2D6* has also been compared to data from targeted Illumina NGS in 17 individuals (Fukunaga et al., 2021). These 17 included one hybrid haplotype (*CYP2D6*36*), including a duplication thereof and its occurrence together with *CYP2D6*10* in a hybrid tandem (*CYP2D6*36+*10*). A recent study has applied the HiFi SMRT technology to 561 patients treated with tamoxifen, and to separate cohorts treated with tamoxifen and venlafaxine (van der Lee et al., 2021). In the tamoxifen-treated dataset, only four individuals with hybrids were identified by the SMRT, and the hybrid haplotype was not specified (Supplementary Table S2; van der Lee et al.,

bioRxiv preprint doi: https://doi.org/10.1101/2022.08.17.503990; this version posted August 18, 2022. The copyright holder for this preprint (which was not certified by peer review) is the author/funder. All rights reserved. No reuse allowed without permission.

2021). The latest relevant SMRT paper used a long-range polymerase chain reaction (L-PCR) technique that amplified a 6.1 kb region spanning from 712 bp upstream to 1176 bp downstream of the NB_008376.4 *CYP2D6* RefSeq coding sequence, and, in addition (by design), amplified the corresponding region from *CYP2D7*, generating a 7.6 kb amplicon in an analysis of 377 Solomon Islanders (Charnaud et al., 2022). From the SMRT data, 27/365 (7.6%) samples appeared to have a *CYP2D6-2D7* fusion haplotype with breakpoints in exon 8 (consistent with a *CYP2D6*63*), and 7/365 (2%) samples appeared to have *CYP2D7-2D6* fusions (*CYP2D6*13*). However, there was a degree of discrepancy between the above and TaqMan CNV intron 9 and exon 9 data, with not all of the samples with a *CYP2D6-2D7* predicted fusion haplotype having a higher intron 2 than exon 9 CNV count, and 1/7 of the predicted *CYP2D7-2D6* fusions not having a high exon 9 count. In addition, the upstream region covered was insufficient for submission of novel haplotypes to PharmVar, which requires at least 1600 bp upstream of the ATG start sequence (to cover the -1584C/G SNP).

The research gap that we address herein is therefore: creating an efficient and accurate HiFi SMRT amplicon-based method capable of detecting the full range of *CYP2D6-2D7* and *CYP2D7-2D6* fusion genes.

Methods

Samples

Used herein was the subset of 95 DNA samples from patients with depression in the Genome-based therapeutic drugs for depression (GENDEP) pharmacogenomics clinical trial as previously described (Carvalho Henriques et al., 2021b), specifically, the 19 samples with *CYP2D6* hybrid haplotypes, plus one additional putative hybrid identified by TaqMan copy number variant (CNV) screening using the methodology described by Carvalho Henriques et al. (2021b). GENDEP was designed to identify pharmacogenomic predictors of response to two antidepressants, nortriptyline and escitalopram, the metabolism of which both involve CYP2D6 (Carvalho Henriques et al., 2020b). DNA was extracted from venous blood. The 19 samples had prior data from multiple technologies (the AmpliChip CYP450 test, TaqMan SNV and CNV data, the Ion AmpliSeq Pharmacogenomics Panel, PharmacoScan, and Sanger sequencing) resulting in consensus genotype calls, while the one additional sample had only prior AmpliChip CYP450 (*CYP2D6*1/*2*) and TaqMan CNV data that were unequal across different regions of *CYP2D6*

bioRxiv preprint doi: https://doi.org/10.1101/2022.08.17.503990; this version posted August 18, 2022. The copyright holder for this preprint (which was not certified by peer review) is the author/funder. All rights reserved. No reuse allowed without permission.

(intron 2, intron 6, and exon 9 calls of 3, 3, and 2, respectively), indicating the presence of a *CYP2D6-2D7* fusion gene. In total, there were 20 samples, two of which had consensus genotypes consistent with two hybrid haplotypes. In addition, we used two samples from the Genetic Testing Reference Material Program (GeT-RM) collection as positive controls for *CYP2D6-2D7* (NA18545, *CYP2D6*5/*36x2+*10x2*) and *CYP2D7-2D6 (*NA19785*, CYP2D6*1/*13+*2)* hybrid haplotypes, respectively (Gaedigk et al., 2019).

L-PCRs using barcoded universal primers for multiplexing amplicons

We adapted protocols for amplifying hybrid-specific amplicons E, G, and H as described (Kramer et al., 2009; Gaedigk et al., 2010b; Black et al., 2012; Carvalho Henriques et al., 2021b) for the PacBio barcoded universal primers for multiplexing amplicons method (PacBio, 2020). A 5' universal sequence and a 5' amino modifier C6 (5AmMC6, to prevent unbarcoded amplicons from being sequenced) were added to each primer (Supplementary Table S1, Thermo Fisher Scientific) for the first-round L-PCR.

First-Round L-PCRs were performed using KAPA HiFi HotStart ReadyMix (Roche Molecular Systems). Reactions (50 µl, in duplicate) contained primers at 0.3 µM each, dNTPs at 0.6 µM, $MgCl_2$ at 2.75 µM, 2% DMSO, and 3 µl of template at 25-202 ng/ µl (more template was used for samples previously showing a relatively low amplicon generating efficiency). For the E amplicon, DNA was amplified for 30 cycles with denaturation at 98°C for 30 s, cycling at 98°C for 10 s, annealing at 85°C for 30 s, and extension at 73°C for 7.5 min (latterly adjusted to 8 min), followed by a terminal extension step of 73°C for 10 min. For the G amplicon, conditions were: denaturation at 98°C for 30 s; 30 cycles of 98°C for 10 s, and annealing and extension at 72°C for 6 min; followed by a terminal extension step of 72°C for 7 min. For the H amplicon, conditions were: denaturation at 95°C; 35 cycles of 98°C for 20 s, annealing at 74°C for 30 s and extension at 73°C for 5 min; followed by a terminal extension step of 72°C for 10 min.

PCR products were visualized on a 1% agarose gel, quantified using the Qubit dsDNA HS assay using a Qubit 3.0 Fluorometer (Thermo Fisher Scientific), and visualized using an Agilent DNA 12000 kit on an Agilent 2100 Bioanalyzer (Agilent Technologies) (Figure 2). As some nonspecific products and primer oligomers were seen on the Agilent output for amplicons E and H, respectively, size selection using AMPure PB Beads (PacBio) was used. Purified sample and

bioRxiv preprint doi: https://doi.org/10.1101/2022.08.17.503990; this version posted August 18, 2022. The copyright holder for this preprint (which was not certified by peer review) is the author/funder. All rights reserved. No reuse allowed without permission.

peak concentrations were measured with the Qubit dsDNA HS and Agilent DNA 12000 assays, respectively.

In the second-round L-PCR, barcoded universal primers (barcoded universal F/R primers plate 96 v2, PacBio) were attached to the forward and reverse universal sequences in the amplicons from the first-round L-PCR. Reactions (25 µl, in duplicate or more, using KAPA HiFi HotStart ReadyMix) contained 2.5 µl barcoded primers, dNTPs at 0.6 µM, $MgCl_2$ at 2.75 µM, 2% DMSO, and 1.5-3 ng template. For the E amplicons, cycling conditions were the same as those used in the first-round L-PCR, with reduction in the number of cycles to 20. For the G amplicons, conditions were: denaturation at 98°C for 30 s; followed by 30 cycles of 98°C for 10 s, annealing at 70°C for 15 s, and extension 72°C for 6 min; then a terminal extension step at 72°C for 7 min. Conditions for the H amplicon were: denaturation at 98°C; 35 cycles of 98°C for 20s, annealing at 74°C for 30 s and extension at 73°C for 5 min; followed by a terminal extension step at 72°C for 10 min. After quantification of amplicons using the same methods as for the first-round, size selection and removal of excess primers was conducted using AMPure PB Beads (PacBio).

Samples were pooled in equimolar amounts (~23 fmol), calculated using approximations of estimated amplicon lengths and the NEBioCalculator (New England Bio Labs), to generate a pool mass of 1-2 µg, with size selection using AMPure PB Beads of the pool, and visualization using the Agilent DNA 12000 kit (Figure 3).

Sequencing

SMRTbell library construction using a pool input mass of 2 µg following visualization using an Agilent TapeStation, size selection using AMPure PB Beads, sequencing with a 30 hour movie time on an 8M cell using the Sequel IIe platform were conducted at The Centre for Applied Genomics (TCAG), the Hospital for Sick Children, Toronto, Canada. Data demultiplexing, resulting in files with extensions of bam, bam.pbi, and consensusreadset, was conducted by the bioinformatics team at TCAG.

Data Analysis and Sequence Alignment

After filtering CCS reads based on amplicon length, alignment versus reference sequences was conducted using SMRT Link Software version 10.2. Reference sequences (from National Center

bioRxiv preprint doi: https://doi.org/10.1101/2022.08.17.503990; this version posted August 18, 2022. The copyright holder for this preprint (which was not certified by peer review) is the author/funder. All rights reserved. No reuse allowed without permission.

for Biotechnology Information (NCBI) or PharmVar) for alignment were deduced from the consensus genotypes previously generated (Supplementary Table S1).

Results

Amplicons from twenty-one hybrid haplotypes were submitted (for one sample with two types of hybrids, only one was submitted) for sequencing, plus three positive controls. Data from twenty-three hybrid haplotypes passed quality control and were analyzed including positive controls (13 E, 8 G, and two H) (Tables 1-3). The E amplicons aligned to **36*, **63*, and **68* hybrid haplotypes as well as to sequences of the various hybrid haplotypes that have the 1847G>A (splice defect) SNV that is the defining SNV for the **4* haplotypes (Table 1). The latter include EU530605 (**4-like*; Kramer et al., 2009), EU530604 (**4N*; Kramer et al., 2009), and PV00250 (PharmVar **4.013*). Alignments against all three prior known **4* hybrid haplotypes are presented (Table 1) for the relevant amplicons apart from one, for which alignment against PV00250 was not possible (sample 5). For the aligned E and G amplicons, 8/13 (61.5%; Table 1) and 5/8 (62.5%; or 6/9=66.6% including the technical replicate, Table 2), respectively, had a percentage alignment above 99% against at least one reference sequence. For the H amplicons (the least abundant size moiety in the pool), the alignments were above 97% (Table 3).

Discussion

In summary, we were able to develop and optimize an amplicon-based method of detecting a range of *CYP2D6-2D7* and *CYP2D7-2D6* fusion genes using PacBio barcoded universal primers (BUP) for multiplexing amplicons. This is the most challenging type of *CYP2D6* variant to detect and characterize. Data analysis was highly efficient (taking a matter of minutes). Data were cross-validated versus previous data from multiple technologies (Carvalho Henriques et al., 2021b), and many of the resulting percentage alignments were above 99%. This method would therefore appear to be more accurate and efficient than any of the other SMRT HiFi methodologies reported to date (Fukunaga et al., 2021; van der Lee et al., 2021; Charnaud et al., 2022) for the detection and characterization of *CYP2D6* fusion genes. In addition, we have since used the forward primer for the E amplicon and the reverse primer for the G amplicon to generate an L-PCR product for non-hybrid *CYP2D6* haplotypes (data not shown). Therefore, the combination of four primer pairs (E forward, E reverse, G forward, G reverse) is sufficient for an amplicon-based method of *CYP2D6*

bioRxiv preprint doi: https://doi.org/10.1101/2022.08.17.503990; this version posted August 18, 2022. The copyright holder for this preprint (which was not certified by peer review) is the author/funder. All rights reserved. No reuse allowed without permission.

characterization apart from a minority of *CYP2D7-2D6* hybrids for which the H amplicon appears to be required. Moreover, the E forward primer is 1909 base pairs (bp) upstream from the ATG start site, and the G reverse primer 619 bp downstream from the TAG stop site. The amplicon generated therefore covers the upstream (to -1600 bp) and downstream (to 265 bp) regions required for novel haplotype submission to PharmVar.

For several G amplicons, the alignment was particularly good, with a relatively low number of differences between the aligned CCS and the reference sequence. There may be at least two potential reasons for this. Firstly, in the first-round L-PCRs for the Gs, we were able to generate amplicons with minimal non-specificity. Secondly, a **13* haplotype was the first type of *CYP2D6* fusion gene to be identified (Daly et al., 1996), and hence has been relatively well studied since (with there now being 10 publicly available sequences) in comparison to the other hybrid haplotypes.

Within the E amplicon group, the variable alignment statistics for hybrid haplotypes in the **4* hybrid haplotypes may reflect the fact that (like the various **13* hybrid haplotypes; PharmVar 2022b) this is a family of hybrid haplotypes containing the 1847G>A SNV. For samples 5, 6 and 16, the alignments being comparable for the prior known **4* hybrid haplotypes and less than 98% may reflect either the need for better optimization of the E amplicon procedure, or that these samples in fact have a previously unreported **4* hybrid haplotype. For the samples with a **36* haplotype, the alignment statistics for the **36* core haplotype and various subhaplotyes were comparable. Sample NA18545 has not previously been sequenced, with the genotype being deduced from CNV testing using L-PCR and quantitative CNV analysis (Gaedigk, personal communication). At present the percentage alignments to the core **36* haplotype and four subhaplotypes presented is too similar to be able to discern which **36* subhaplotype is present (and, conceivably, as this sample has a **36* duplication, it may have more than one **36* subhaplotype). Further optimization of the E amplicon procedure as below may resolve this. The sample with a **68* haplotype aligned best to EU530606, with the alignment to the other **68* partial reference sequence (JF307779) being only 87.5%. The sample with a **63* haplotype had a percentage alignment that may again either reflect need for greater optimization, or potentially the presence of a slightly different haplotype than that previously reported. Of note, our E amplicons were longer (by ~1.7 kb) than previously described (Kramer et al., 2009; Black et al., 2012). Initial setting of the extension time in the cycling parameters reflected the shorter predicted length, and

bioRxiv preprint doi: https://doi.org/10.1101/2022.08.17.503990; this version posted August 18, 2022. The copyright holder for this preprint (which was not certified by peer review) is the author/funder. All rights reserved. No reuse allowed without permission.

while we subsequently set extension to 8 min, this could likely be further optimized to 8.5 min. Accurate amplicon sizing is important not only for L-PCR optimization but also for molar calculations in amplicon pooling.

The percentage alignment being less (97.0-98.3%) for the H amplicons may well reflect the lower abundance of that amplicon in the pool. One of the H amplicons aligned best to haplotypes **13C*, **13D* and **13E*. Prior Sanger sequencing data for one of our hybrids was consistent with a **13* haplotype with a switch region such that the possible haplotypes were **13C*, **13D*, or **13E*. The SMRT data are therefore consistent with the Sanger sequencing data, but not yet robust enough to delineate between the three possible subhaplotypes. Of note, we have identified a step in the cycling parameters that can be optimized. We are therefore in the process of repeating the HiFi sequencing. The other H amplicon (NA19785, *CYP2D6* genotype **1/*13+*2*; Gaedigk et al., 2019) had comparable alignments to **13A1*, **13A2* and **13B*. The prior sequence aligns to **13A2* (Gaedigk, personal communication). We are also repeating the HiFi sequencing of this amplicon.

Owing to the presence of some non-specific products at less than the correct length resulting from E L-PCRs, size selection to remove products less than ~3 kb was conducted using AMPure PB beads. Whilst the final pool profile indicates the persistence of such products, HiFi sequencing was nonetheless able to produce alignments for all but one of the amplicons supplied. This may be at least partly attributable to the relatively small number of multiplexed amplicons, resulting in a high degree of redundancy and read depth. However, the accuracy of less than 99% for some of our amplicons may reflect the need for a greater degree of optimization of the technique, particularly for the E amplicons (currently underway).

The main limitation of the work reported herein is the variable percentage alignments, some of which may reflect factors such as PCR optimization achieved by the time of sequence submission. The alignment previously achieved by Sanger sequencing was slightly higher than that achieved by SMRT (e.g., sample 33, alignment 100%; sample 5, alignment 99.75% to **4-like*). This was, however, after manual curation of the Sanger sequencing data (e.g., if two pieces of sequencing data were concordant with the reference and one was not, the one discordant read was not counted). The SMRT alignment process was automated. Moreover, the entire SMRT process reported herein is much more efficient than Sanger sequencing.

bioRxiv preprint doi: https://doi.org/10.1101/2022.08.17.503990; this version posted August 18, 2022. The copyright holder for this preprint (which was not certified by peer review) is the author/funder. All rights reserved. No reuse allowed without permission.

This is the first report of an amplicon-based method of *CYP2D6* SMRT sequencing on a range of fusion genes with haplotypes previously characterized by multiple technologies. Although some versions of *CYP2D6-2D7* fusion genes (e.g., *CYP2D6*61*) were not in our sample set, we are not aware of any reason for our method not working for any *CYP2D6-2D7* fusion gene.

Although CYP2D6 plays a key role in the metabolism of ~20-25% of clinically used drugs (Ingelman-Sundberg, 2005; Zanger et al., 2013), and is included in drug labelling by regulatory bodies (the U.S. Food and Drug Administration, the European Medicines Agency, the Pharmaceuticals and Medical Devices Agency) and prescribing recommendations by consortia (Clinical Pharmacogenetics Implementation Consortium, the Dutch Pharmacogenetics Working Group), identification of *CYP2D6* variants is not yet routine in clinical practice. This is despite the fact that dispensing data indicate that many patients are being prescribed medications for which the identification of *CYP2D6* variants prior to these medications being dispensed could be helpful (Fan et al., 2021) One of the reasons for this is the complexity of the locus, and in particular the fact that the fusion genes are challenging to identify and accurately characterize. Another reason is that clinical implementation requires an efficient, high throughput method that requires relatively little personnel time. The HiFi sequencing method reported herein is suitable for high throughput, efficient, with accurate characterization of the full range of *CYP2D6* haplotypes, and can be completed in a week or less. Moreover, the method that we have developed could be extended (particularly for other complex loci with structural variants). In this manner a group of genes may be efficiently characterized in a multiplexed high throughput assay.

Acknowledgements

We thank the University of Alberta Faculty of Medicine and Dentistry High Content Analysis Core and Department of Experimental Oncology for access to instrumentation and/or, and the University of Alberta Department of Biological Sciences Molecular Biology Service Unit (MBSU) for Sanger sequencing (contribution to data in Supplementary Table S1). We thank Andrea Gaedigk for personal communications regarding the details of GeT-RM samples NA19785 and NA18545 used in this report. The work described in this paper was funded by: a Canada Foundation for Innovation (CFI), John R. Evans Leaders Fund (JELF) grant (32147—Pharmacogenetic translational biomarker discovery, to KJA), an Alberta Innovates Strategic Research Project (SRP51_PRIME - Pharmacogenomics for the Prevention of Adverse Drug

bioRxiv preprint doi: https://doi.org/10.1101/2022.08.17.503990; this version posted August 18, 2022. The copyright holder for this preprint (which was not certified by peer review) is the author/funder. All rights reserved. No reuse allowed without permission.

Reactions in mental health; G2018000868 to KJA and Chad Bousman), an Alberta Centennial Addiction and Mental Health Research Chair (to KJA), an Alberta Innovation and Advanced Education Small Equipment Grant (to KJA), the Department of Psychiatry, and the Faculty of Medicine and Dentistry at the University of Alberta. The infrastructure from GP's lab for the running of the Ion AmpliSeq Pharmacogenomics Panel was supported by a Hotchkiss Brain Institute Dementia Equipment Fund grant (to CB and GP for the Ion) and a Canada Foundation for Innovation John R. Evans Leaders Fund Grant (CFI-JELF) (36624 - Neuromuscular genetics program, to GP). GENDEP was funded by a European Commission Framework 6 grant, LSHB-CT-2003-503428. Roche Molecular Systems supplied the AmpliChip CYP450 Test arrays and some associated support. GlaxoSmithKline and the Medical Research Council (UK) contributed by funding add-on projects in the London centre. This paper is an original work and the views expressed here can only be attributed to the authors, not necessarily reflecting those of the NHS, the NIHR or the UK Department of Health and Social Care.

bioRxiv preprint doi: https://doi.org/10.1101/2022.08.17.503990; this version posted August 18, 2022. The copyright holder for this preprint (which was not certified by peer review) is the author/funder. All rights reserved. No reuse allowed without permission.

References

Aitchison KJ, Munro J, Wright P, Smith S, Makoff AJ, Sachse C, Sham PC, Murray RM, Collier DA, Kerwin RW (1999) Failure to respond to treatment with typical antipsychotics is not associated with CYP2D6 ultrarapid hydroxylation. British Journal of Clinical Pharmacology.

Aitchison KJ, Gill M (2002) Pharmacogenetics in the Postgenomic Era. In: Behavioral Genetics in the Postgenomic Era. (Plomin R, DeFries J, Craig I, McGuffin P, eds). Washington, DC: American Psychological Association.

Aitchison K, Datla K, Rooprai H, Fernando J, Dexter D (2009) Regional distribution of clomipramine and desmethylclomipramine in rat brain and peripheral organs on chronic clomipramine administration. Journal of Psychopharmacology 24:1261-1268.

Altar CA, Hornberger J, Shewade A, Cruz V, Garrison J, Mrazek D (2013) Clinical validity of cytochrome P450 metabolism and serotonin gene variants in psychiatric pharmacotherapy. International Review of Psychiatry 25:509–533.

Ameur A, Kloosterman WP, Hestand MS (2019) Single-Molecule Sequencing: Towards Clinical Applications. Trends in Biotechnology 37:72–85 Available at: https://www.sciencedirect.com/science/article/pii/S016777991830204X.

Ardui S, Ameur A, Vermeesch JR, Hestand MS (2018) Single molecule real-time (SMRT) sequencing comes of age: Applications and utilities for medical diagnostics. Nucleic Acids Research 46:2159–2168.

Benjamini Y, Speed TP (2012) Summarizing and correcting the GC content bias in high-throughput sequencing. Nucleic Acids Research 40.

Bertilsson L, Alm C, De Las Carreras C, Widen J, Edman G, Schalling D (1989) Debrisoquine hydroxylation polymorphism and personality. Lancet 1:555

Bertilsson L, Dahl M-L, Al-Shurbaji A (2002) Molecular genetics of CYP2D6: Clinical relevance with focus on psychotropic drugs. Available at: www.imm.ki.se/CYPalleles/cyp2d6.htm.

bioRxiv preprint doi: https://doi.org/10.1101/2022.08.17.503990; this version posted August 18, 2022. The copyright holder for this preprint (which was not certified by peer review) is the author/funder. All rights reserved. No reuse allowed without permission.

Black JL, Walker DL, O'Kane DJ, Harmandayan M (2012) Frequency of undetected CYP2D6 hybrid genes in clinical samples: Impact on phenotype prediction. Drug Metabolism and Disposition 40:111–119.

Bousman CA, Bengesser SA, Aitchison KJ, Amare AT, Aschauer H, Baune BT, Asl BB, Bishop JR, Burmeister M, Chaumette B, Chen L, Cordner ZA, Deckert J, Degenhardt F, DeLisi LE, Folkersen L, Kennedy JL, Klein TE, McClay JL, McMahon FJ, Musil R, Saccone NL, Sangkuhl K, Stowe RM, Tan E, Tiwari AK, Zai CC, Zai G, Zhang J, Gaedigk A, Muller DJ (2021) Review and Consensus on Pharmacogenomic Testing in Psychiatry. Pharmacopsychiatry 54:5–17.

Buermans HPJ, Vossen RHAM, Anvar SY, Allard WG, Guchelaar HJ, White SJ, den Dunnen JT, Swen JJ, van der Straaten T (2017) Flexible and Scalable Full-Length CYP2D6 Long Amplicon PacBio Sequencing. Human Mutation 38:310–316.

Carvalho Henriques B, Buchner A, Hu X, Yavorskyy V, Wang Y, Martens K, Carr M, Asl BB, Hague J, Maier W, Dernovsek MZ, Henigsberg N, Souery D, Cattaneo A, Hauser J, Mors O, Rietschel M, Pfeffer G, Bousman C, Aitchison KJ (2020a) Cross-validation of technologies for genotyping CYP2D6 and CYP2C19. bioRxiv. https://doi.org/10.1101/2019.12.24.870295

Carvalho Henriques B, Lapetina D, Yavorskyy V, Carr M, Hague J, Aitchison KJ (2020b) How can drug metabolism and transporter genetics inform psychotropic prescribing? Frontiers in Genetics 11. https://doi.org/10.3389/fgene.2020.491895

Carvalho Henriques B, Buchner A, Hu X, Wang Y, Yavorskyy V, Dong R, Martens K, Carr M, Asl BB, Wallace K, Hague J, Sivapalan S, Maier W, Dernovsek MZ, Henigsberg N, Hauser J, Souery D, Cattaneo A, Mors O, Rietschel M, Pfeffer G, Bousman C, Aitchison KJ (2021a) Validation of methodology for efficient genotyping of CYP2D6 and CYP2C19. Research Square:1–13. https://doi.org/10.21203/rs.3.rs-123677/v1

Carvalho Henriques B, Buchner A, Hu X, Wang Y, Yavorskyy V, Wallace K, Dong R, Martens K, Carr M, Asl BB, Hague J, Sivapalan S, Maier W, Dernovsek MZ, Henigsberg N, Hauser J, Souery D, Cattaneo A, Mors O, Rietschel M, Pfeffer G, Huma S, Aitchison KJ (2021b) Methodology for clinical genotyping of CYP2D6 and CYP2C19. Translational Psychiatry 11. https://doi.org/10.1038/s41398-021-01717-9

bioRxiv preprint doi: https://doi.org/10.1101/2022.08.17.503990; this version posted August 18, 2022. The copyright holder for this preprint (which was not certified by peer review) is the author/funder. All rights reserved. No reuse allowed without permission.

Caudle KE, Sangkuhl K, Whirl-Carrillo M, Swen JJ, Haidar CE, Klein TE, Gammal RS, Relling M v, Scott SA, Hertz DL, Guchelaar H-J, Gaedigk A (2020) Standardizing CYP2D6 Genotype to Phenotype Translation: Consensus Recommendations from the Clinical Pharmacogenetics Implementation Consortium and Dutch Pharmacogenetics Working Group. Clin Transl Sci 13:116–124.

Charnaud S, Munro JE, Semenec L, Mazhari R, Brewster J, Bourke C, Ruybal-Pesántez S, James R, Lautu-Gumal D, Karunajeewa H, Mueller I, Bahlo M (2022) PacBio long-read amplicon sequencing enables scalable high-resolution population allele typing of the complex CYP2D6 locus. Communications Biology 5:168 Available at: https://doi.org/10.1038/s42003-022-03102-8.

Cheng J, Zhen Y, Miksys S, Beyoglu D, Krausz KW, Tyndale RF, Yu AM, Idle JR, Gonzalez FJ (2013) Potential role of CYP2D6 in the central nervous system. Xenobiotica: The Fate of Foreign Compounds in Biological Systems 43:973-84.

Crews KR, Monte AA, Huddart R, Caudle KE, Kharasch ED, Gaedigk A, Dunnenberger HM, Leeder JS, Callaghan JT, Samer CF, Klein TE, Haidar CE, Van Driest SL, Ruano G, Sangkuhl K, Cavallari LH, Muller DJ, Prows CA, Nagy M, Somogyi AA, Skaar TC (2021) Clinical Pharmacogenetics Implementation Consortium Guideline for CYP2D6, OPRM1, and COMT Genotypes and Select Opioid Therapy. Clinical Pharmacology and Therapeutics 110:888-896.

Dalton R, Lee S been, Claw KG, Prasad B, Phillips BR, Shen DD, Wong LH, Fade M, McDonald MG, Dunham MJ, Fowler DM, Rettie AE, Schuetz E, Thornton TA, Nickerson DA, Gaedigk A, Thummel KE, Woodahl EL (2020) Interrogation of CYP2D6 Structural Variant Alleles Improves the Correlation Between CYP2D6 Genotype and CYP2D6-Mediated Metabolic Activity. Clinical and Translational Science 13:147–156.Daly AK, Fairbrother KS, Andreassen OA, London SJ, Idle JR, Steen VM (1996) Characterization and PCR-based detection of two different hybrid CYP2D7P/CYP2D6 alleles associated with the poor metabolizer phenotype. Pharmacogenetics 6:319-28.

Danielson P (2005) The Cytochrome P450 Superfamily: Biochemistry, Evolution and Drug Metabolism in Humans. Current Drug Metabolism 3:561–597.

bioRxiv preprint doi: https://doi.org/10.1101/2022.08.17.503990; this version posted August 18, 2022. The copyright holder for this preprint (which was not certified by peer review) is the author/funder. All rights reserved. No reuse allowed without permission.

Ekholm J (2017) Long-read sequencing offers path to more accurate drug metabolism profiles. Drug Discovery World 18:24–28.

Fan M, Yarema MC, Box A, Hume S, Aitchison KJ, Bousman CA (2021) Identification of high-impact gene-drug pairs for pharmacogenetic testing in Alberta, Canada. Pharmacogenetics and Genomics:29–39.

Fukunaga K, Hishinuma E, Hiratsuka M, Kato K, Okusaka T, Saito T, Ikeda M, Yoshida T, Zembutsu H, Iwata N, Mushiroda T (2021) Determination of novel CYP2D6 haplotype using the targeted sequencing followed by the long-read sequencing and the functional characterization in the Japanese population. Journal of Human Genetics 66:139–149 Available at: http://dx.doi.org/10.1038/s10038-020-0815-x.

Funae Y, Kishimoto W, Cho T, Niwa T, Hiroi T (2003) CYP2D in the brain. Drug Metab Gaedigk A, Coetsee C (2008) The CYP2D6 gene locus in South African Coloureds: unique allele distributions, novel alleles and gene arrangements. European Journal of Clinical Pharmacology 64:465-75.olism and Pharmacokinetics 18:337-49.

Gaedigk A, Coetsee C (2008) The CYP2D6 gene locus in South African Coloureds: unique allele distributions, novel alleles and gene arrangements. European Journal of Clinical Pharmacology 64:465-75.

Gaedigk A, Fuhr U, Johnson C, Bérard LA, Bradford DA, Leeder JS (2010a) CYP2D7-2D6 hybrid tandems: Identification of novel CYP2D6 duplication arrangements and implications for phenotype prediction. Pharmacogenomics 11:43–53.

Gaedigk A, Jaime LKM, Bertino JS, Bérard A, Pratt VM, Bradford LDA, Leeder JS (2010b) Identification of novel CYP2D7-2D6 hybrids: Non-functional and functional variants. Frontiers in Pharmacology OCT.

Gaedigk A (2013) Complexities of CYP2D6 gene analysis and interpretation. International Review of Psychiatry 25:534–553.

Gaedigk A, Riffel AK, Berrocal BG, Solaesa VG, Dávila I, Isidoro-García M (2014) Characterization of a complex CYP2D6 genotype that caused an AmpliChip CYP450 Test® no-call in the clinical setting. Clinical Chemistry and Laboratory Medicine 52:799–807.

bioRxiv preprint doi: https://doi.org/10.1101/2022.08.17.503990; this version posted August 18, 2022. The copyright holder for this preprint (which was not certified by peer review) is the author/funder. All rights reserved. No reuse allowed without permission.

Gaedigk A, Ingelman-Sundberg M, Miller NA, Leeder JS, Whirl-Carrillo M, Klein TE (2018) The Pharmacogene Variation (PharmVar) Consortium: Incorporation of the Human Cytochrome P450 (CYP) Allele Nomenclature Database. Clin Pharmacol Ther 103:399–401.

Gaedigk A, Turner A, Everts RE, Scott SA, Aggarwal P, Broeckel U, McMillin GA, Melis R, Boone EC, Pratt VM, Kalman LV (2019) Characterization of Reference Materials for Genetic Testing for CYP2D6 Alleles: A GeT-RM Collaborative Project. J Mol Diagn 21(6):1034-1052

Gan SH, Ismail R, Wan Adnan WA, Zulmi W, Kumaraswamy N, Larmie ET (2004) Relationship between Type A and B personality and debrisoquine hydroxylation capacity. British Journal of Clinical Pharmacology 57:785–789

Gonzalez FJ (2008) Regulation of hepatocyte nuclear factor 4 alpha-mediated transcription. Drug Metabolism and Pharmacokinetics 23:2–7.

GTEx Portal (2021) CYP2D6 Gene Page. Available at https://www.gtexportal.org/home/gene/ENSG00000100197 [Accessed Aug 6, 2022]

Han DD, Gu HH (2006) Comparison of the monoamine transporters from human and mouse in their sensitivities to psychostimulant drugs. BMC Pharmacology 6:6.

Heather JM, Chain B (2016) The sequence of sequencers: The history of sequencing DNA. Genomics 107:1–8.

Hiroi T, Imaoka S, Funae Y (1998) Dopamine Formation from Tyramine by CYP2D6. Biochemical and Biophysical Research Communications 249:838-843.

Howes OD, Thase ME, Pillinger T (2021) Treatment resistance in psychiatry: state of the art and new directions. Molecular Psychiatry.

Ingelman-Sundberg M (2005) Genetic polymorphisms of cytochrome P450 2D6 (CYP2D6): clinical consequences, evolutionary aspects and functional diversity. The Pharmacogenomics Journal 5:6-13.

bioRxiv preprint doi: https://doi.org/10.1101/2022.08.17.503990; this version posted August 18, 2022. The copyright holder for this preprint (which was not certified by peer review) is the author/funder. All rights reserved. No reuse allowed without permission.

Jarvis JP, Peter AP, Shaman JA (2019) Consequences of CYP2D6 Copy-number variation for pharmacogenomics in psychiatry. Frontiers in Psychiatry 10.

Jukic MM, Smith RL, Molden E, Ingelman-Sundberg M (2021) Evaluation of the CYP2D6 Haplotype Activity Scores Based on Metabolic Ratios of 4,700 Patients Treated With Three Different CYP2D6 Substrates. Clinical Pharmacology and Therapeutics 110:750-58

Kimura S, Umeno M, Skodaj RC, Meyert UA, Gonzalez FJ (1989) The Human Debrisoquine 4-Hydroxylase (CYP2D) Locus: Sequence and Identification of the Polymorphic CYP2D6 Gene, a Related Gene, and a Pseudogene.

Kramer WE, Walker DL, O'Kane DJ, Mrazek DA, Fisher PK, Dukek BA, Bruflat JK, Black JL (2009) CYP2D6: Novel genomic structures and alleles. Pharmacogenetics and Genomics 19:813–822.

Kirchheiner J, Seeringer A, Godoy AL, Ohmle B, Maier C, Beschoner P, Sim EJ, Viviani R (2011) CYP2D6 in the brain: genotype effects on resting brain perfusion. Molecular Psychiatry 16:237, 333-41.

Laver TW, Caswell RC, Moore KA, Poschmann J, Johnson MB, Owens MM, Ellard S, Paszkiewicz KH, Weedon MN (2016) Pitfalls of haplotype phasing from amplicon-based long-read sequencing. Scientific Reports 6:1–6.

Liau Y, Maggo S, Miller AL, Pearson JF, Kennedy MA, Cree SL (2019) Nanopore sequencing of the pharmacogene CYP2D6 allows simultaneous haplotyping and detection of duplications. Pharmacogenomics 20:1033–1047.

Miksys S, Rao Y, Hoffman E, Mash DC, Tyndale RF (2002) Regional and cellular expression of CYP2D6 in human brain: higher levels in alcoholics. Journal of Neurochemistry 82:1376-87.

Miksys SL, Cheung C, Gonzalez FJ, Tyndale RF (2005) Human CYP2D6 and mouse CYP2Ds: Organ distribution in a humanized mouse model. Drug Metabolism and Disposition 33:1495-1502.

Mrazek DA, Hornberger JC, Altar CA, Degtiar I (2014) A review of the clinical, economic, and societal burden of treatment-resistant depression: 1996-2013. Psychiatric Services 65:977–987.

bioRxiv preprint doi: https://doi.org/10.1101/2022.08.17.503990; this version posted August 18, 2022. The copyright holder for this preprint (which was not certified by peer review) is the author/funder. All rights reserved. No reuse allowed without permission.

National Human Genome Research Institute (2014) Haplotype: Talking Glossary of Genetic Terms. Available at: https://www.genome.gov/genetics-glossary/haplotype [Accessed November 17, 2021].

Niwa T, Okada K, Hiroi T, Imaoka S, Narimatsu S, Funae Y (2008) Effect of psychotropic drugs on the 21-hydroxylation of neurosteroids, progesterone and allopregnanolone, catalyzed by rat CYP2D4 and human CYP2D6 in the brain. Biological and Pharmaceutical Bulletin 31:348-51.

Niznik HB, Tyndale RF, Sallee FR, Gonzalez FJ, Hardwick JP, Inaba T, Kalow W (1990) The dopamine transporter and cytochrome P450IID1 (debrisoquine 4-hydroxylase) in brain: Resolution and identification of two distinct [3H]GBR-12935 binding proteins. Archives of Biochemistry and Biophysics 276:424-432.

Pacific Biosciences (2020) Procedure & Checklist - Preparing SMRTbell Libraries using PacBio Barcoded Universal Primers for Multiplexing Amplicons. Available at: https://www.pacb.com/wp-content/uploads/Procedure-Checklist-Preparing-SMRTbell-Libraries-using-PacBio-Barcoded-Universal-Primers-for-Multiplexing-Amplicons.pdf. Part Number 101-791-800 Version 02 (April 2020).

Pan X, Ning M, Jeong H (2017) Transcriptional Regulation of CYP2D6 Expression. Drug Metabolism and Disposition 45:42-48.

Panserat S, Mura C, Gerard N, Vincent-Viry M, Galteau MM, Jacoz-Aigrain E, Krishnamoorthy R (1995) An unequal cross-over event within the CYP2D gene cluster generates a chimeric CYP2D7/CYP2D6 gene which is associated with the poor metabolizer phenotype. British Journal of Clinical Pharmacology 40:361-7.

Patten SB, Williams JVA, Lavorato DH, Wang JL, McDonald K, Bulloch AGM (2015) Descriptive epidemiology of major depressive disorder in Canada in 2012. Canadian Journal of Psychiatry 60:23–30.

Patten SB, Williams JVA, Lavorato DH, Wang JL, McDonald K, Bulloch AGM (2016) Major depression in Canada: What has changed over the past 10 years? Canadian Journal of Psychiatry 61:80–85.

bioRxiv preprint doi: https://doi.org/10.1101/2022.08.17.503990; this version posted August 18, 2022. The copyright holder for this preprint (which was not certified by peer review) is the author/funder. All rights reserved. No reuse allowed without permission.

PharmVar (2022a) CYP2D6 Allele Nomenclature. Available at: https://www.pharmvar.org/gene/CYP2D6 [Accessed Aug 5, 2022].

PharmVar (2022b) CYP2D6 Structural Variation Document. Available at: Pharmacogenetics (PGx) Repository (storyblok.com), accessed August 6, 2022.

Pirmohamed M, James S, Meakin S, Green C, Scott AK, Walley TJ, Farrar K, Park BK, Breckenridge AM (2004) Adverse drug reactions as cause of admission to hospital: Prospective analysis of 18 820 patients. British Medical Journal 329:15–19.

Qiao W, Yang Y, Sebra R, Mendiratta G, Gaedigk A, Desnick RJ, Scott SA (2017) Long-read single-molecule real-time (SMRT) full gene sequencing of cytochrome P450-2D6 (CYP2D6). Physiol Behav 176:139–148.

Roberts RJ, Carneiro MO, Schatz MC (2013) The advantages of SMRT sequencing. Genome Biology 14:405 Available at: https://doi.org/10.1186/gb-2013-14-7-405.

Robinson JT, Thorvaldsdóttir H, Winckler W, Guttman M, Lander ES, Getz G, Mesirov JP (2011) Integrative genomics viewer. Nat Biotechnol 29:24–26.

Rush AJ, Trivedi MH, Wisniewski SR, Nierenberg AA, Stewart JW, Warden D, George Niederehe M, Thase ME, Lavori PW, Lebowitz BD, McGrath PJ, Rosenbaum JF, Sackeim HA, Kupfer DJ, Luther J, Maurizio Fava M (2006) Acute and Longer-Term Outcomes in Depressed Outpatients Requiring One or Several Treatment Steps: A STAR*D Report. Available at: www.star-d.org.

Santomauro DF, Herrera AMM, Shadid J, Zheng P, Ashbaugh C, Pigott DM, Abbafati C, Adolph C, Amlag JO, Aravkin AY, Bang-Jensen BL, Bertolacci GJ, Bloom SS, Castellano R, Castro E, Chakrabarti S, Chattopadhyay J, Cogen RM, Collins JK, Dai X, Dangel WJ, Dapper C, Deen A, Erickson M, Ewald SB, Flaxman AD, Frostad JJ, Fullman N, Giles JR, Giref AZ, Guo G, He J, Helak M, Hulland EN, Idrisov B, Lindstrom A, Linebarger E, Lotufo PA, Lozano R, Magistro B, Malta DC, Mansson JC, Marinho F, Mokdad AH, Monasta L, Naik P, Nomura S, O'Halloran JK, Ostroff SM, Pasovic M, Penberthy L, Reiner Jr RC, Reinke G, Ribeiro ALP, Sholokhov A, Sorensen RJD, Varavikova E, Vo AT, Walcott R, Watson S, Wiysonge CS, Zigler B, Hay SI, Vos T, Murray CJL, Whiteford HA, Ferrari AJ(2021)

bioRxiv preprint doi: https://doi.org/10.1101/2022.08.17.503990; this version posted August 18, 2022. The copyright holder for this preprint (which was not certified by peer review) is the author/funder. All rights reserved. No reuse allowed without permission.

Global prevalence and burden of depressive and anxiety disorders in 204 countries and territories in 2020 due to the COVID-19 pandemic. Lancet 398:1700–1712.

Shen H, He MM, Liu H, Wrighton SA, Wang L, Guo B, Li C (2007) Comparative metabolic capabilities and inhibitory profiles of CYP2D6.1, CYP2D6.10, and CYP2D6.17. Drug Metabolism and Disposition: The Biological Fate of Chemicals 35:1292-300.

Siegle I, Fritz P, Eckhardt K, Zanger UM, Eichelbaum M (2001) Cellular localization and regional distribution of CYP2D6 mRNA and protein expression in human brain. Pharmacogenetics 11:237-45.

UCSC Genome Browser (2017) UCSC Genome Browser assembly ID: hg38; Genome Reference Consortium Human GRCh38.p13 (GCA_000001405.28); Dec. 2013 initial release; Dec. 2017 patch release 1.Human hg38 chr22:42,109,251-42,148,058 UCSC Genome Browser v434, accessed August 6, 2022.

Uher R, Huezo-Diaz P, Perroud N, Smith R, Rietschel M, Mors O, Hauser J, Maier W, Kozel D, Henigsberg N, Barreto M, Placentino A, Dernovsek MZ, Schulze TG, Kalember P, Zobel A, Czerski PM, Larsen ER, Souery D, Giovannini C, Gray JM, Lewis CM, Farmer A, Aitchison KJ, McGuffin P, Craig I (2009) Genetic predictors of response to antidepressants in the GENDEP project. Pharmacogenomics Journal 9:225–233.

van der Lee M, Allard WG, Vossen RHAM, Baak-Pablo RF, Menafra R, Deiman BALM, Deenen MJ, Neven P, Johansson I, Gastaldello S, Ingelman-Sundberg M, Guchelaar HJ, Swen JJ, Anvar SY (2020) A unifying model to predict variable drug response for personalised medicine. bioRxiv 668353:1–20.

van der Lee M, Allard WG, Vossen RHAM, Baak-Pablo RF, Menafra R, Deiman BALM, Deenen MJ, Neven P, Johansson I, Gastaldello S, Ingelman-Sundberg M, Guchelaar H, Swen JJ, Anvar SY (2021) Toward predicting CYP2D6-mediated variable drug response from CYP2D6 gene sequencing data. Science Translational Medicine 13:eabf3637.

van der Lee M, Rowell WJ, Menafra R, Guchelaar H-J, Swen JJ, Anvar SY (2022) Application of long-read sequencing to elucidate complex pharmacogenomic regions: a proof of principle. The Pharmacogenomics Journal 22:75–81.

bioRxiv preprint doi: https://doi.org/10.1101/2022.08.17.503990; this version posted August 18, 2022. The copyright holder for this preprint (which was not certified by peer review) is the author/funder. All rights reserved. No reuse allowed without permission.

Yang Y, Botton MR, Scott ER, Scott SA (2017) Sequencing the CYP2D6 gene: From variant allele discovery to clinical pharmacogenetic testing. Pharmacogenomics 18:673–685.

Yasukochi Y, Satta Y (2011) Evolution of the *CYP2D* gene cluster in humans and four non-human primates. Genes and Genetic Systems 86:109-16.

Yu AM, Idle JR, Byrd LG, Krausz KW, Kupfer A, Gonzalez FJ (2003) Regeneration of serotonin from 5-methoxytryptamine by polymorphic human CYP2D6. Pharmacogenetics 13:173-81.

Yu AM, Idle JR, Herraiz T, Kupfer A, Gonzalez FJ (2003) Screening for endogenous substrates reveals that CYP2D6 is a 5-methoxyindolethylamine O-demethylase. Pharmacogenetics 13:307-19.

Zanger UM, Schwab M (2013) Cytochrome P450 enzymes in drug metabolism: Regulation of gene expression, enzyme activities, and impact of genetic variation. Pharmacology and Therapeutics 138:103–141.

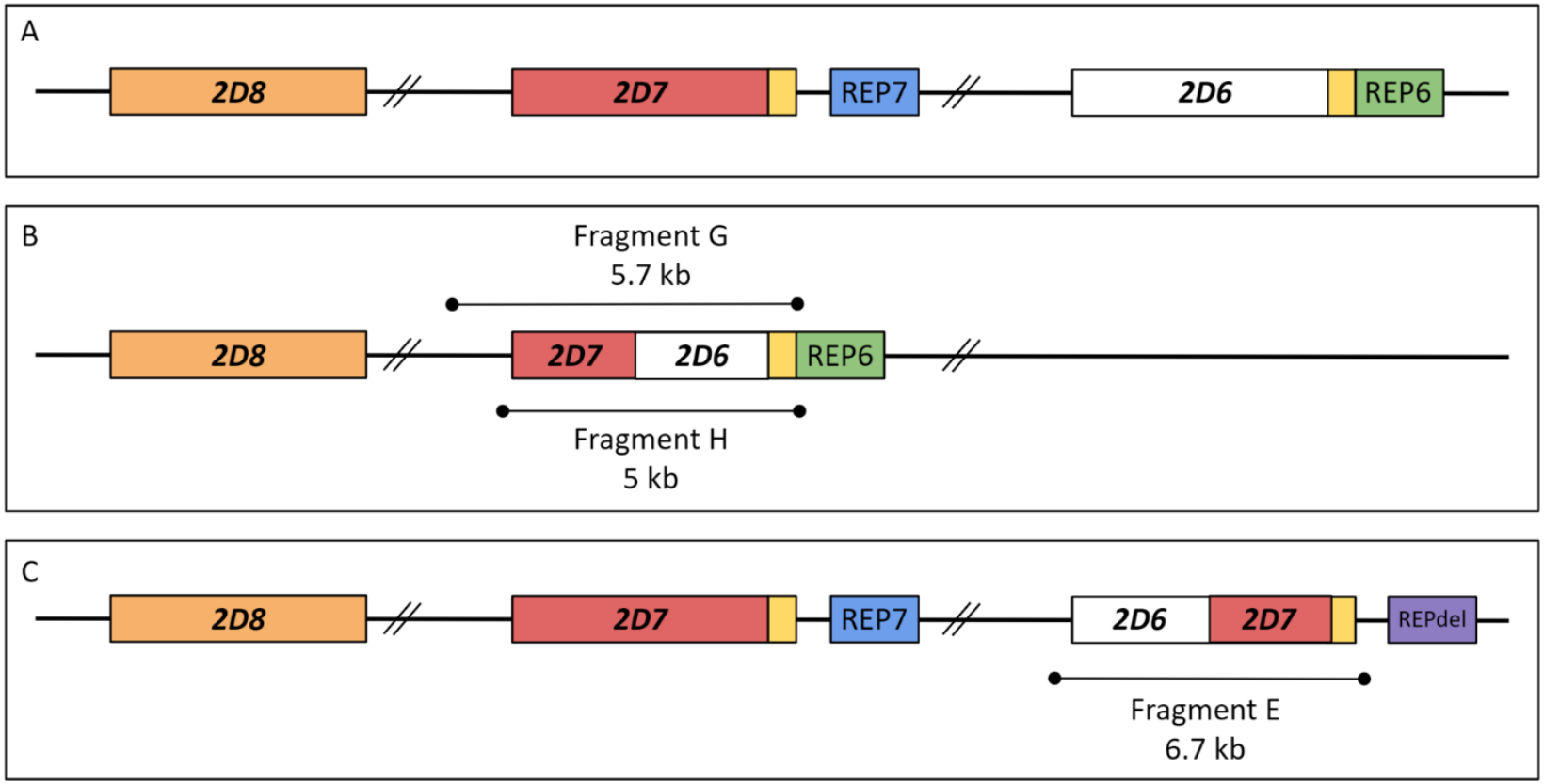

Figure 1. *CYP2D* wild-type locus and fusion genes, with amplicons diagrammed. (**A**) *CYP2D* wild-type locus. (**B**) Example *CYP2D7-2D6* fusion gene. The G and H amplicons are predicted to be 5.7 and 5 kb, respectively (Kramer et al., 2009; Black et al., 2012; Gaedigk et al., 2010b). (**C**) Example *CYP2D6-2D7* fusion gene. The E amplicon is predicted to be 6.7 kb (Kramer et al., 2009; Black et al., 2012).

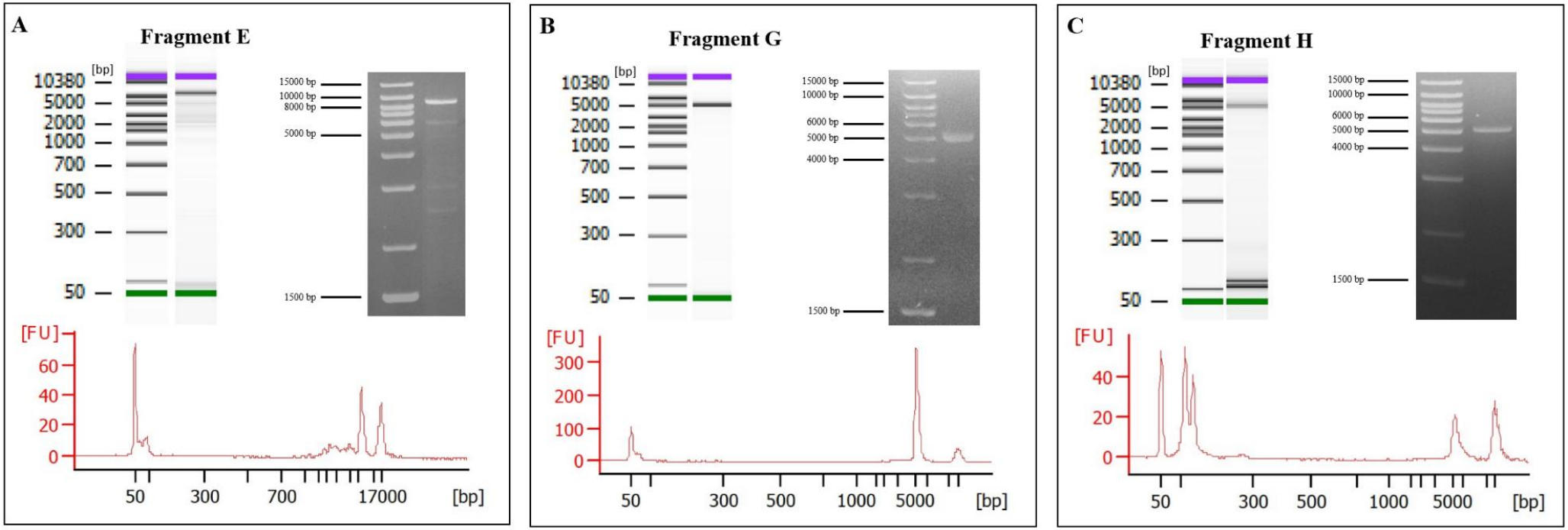

Figure 2. Quality control of first-round L-PCR by agarose gel and Agilent 2100 Bioanalyzer (DNA 12000 assay) electrophoresis. (**A**) Representative E amplicon. (**B**) Representative G amplicon. (**C**) Amplicon H. For the Agilent output, the x-axis indicates length in base pairs (bp) and the y-axis fluorescence intensity in fluorescence units [FU]. The lower marker (50 bp) and upper marker (17000 bp) are the first and last peaks, respectively. Electropherogram plots are transformed into automated gel electrophoresis images (top left), where the bottom marker (green), top marker (purple), and PCR products are visualized alongside the ladder (bp). The 1% agarose gel with a 1 kb Plus DNA Ladder (Thermo Fisher Scientific) is shown in the top right.

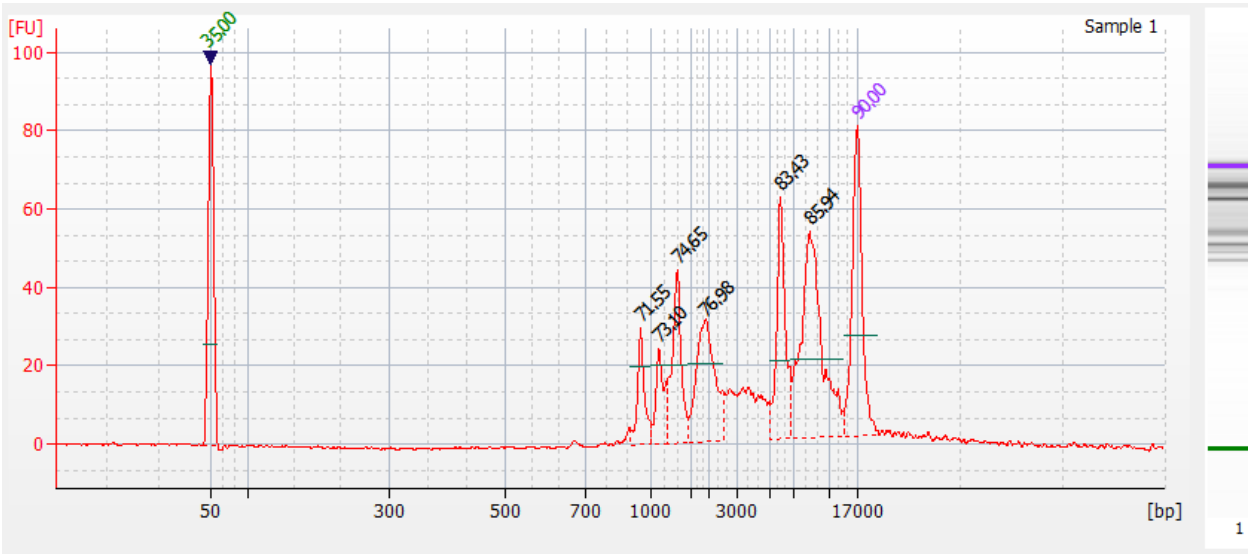

		Size [bp]	Conc. [ng/µl]	Molarity [nmol/l]	Observations
2		953	1.39	2.2	
3		1,100	1.28	1.8	
4		1,328	2.53	2.9	
5		1,876	3.54	2.9	
6		5,876	3.02	0.8	
7		8,448	6.16	1.1	
8	▶	17,000	4.20	0.4	Upper Marker

Figure 3. Sample pool as visualized on the Agilent 1200 assay. The ~5.9 kb peak represents the G amplicons and the ~8.4 kb peak the E amplicons. The H amplicon are hidden in the region between the G peak and the nonspecific lower peaks.

Table 1. Alignment of E amplicons to reference sequences. For the hybrid haplotypes containing the 1847G>A defining SNV for *4, where possible, alignments to all three reference sequences are provided. Sequences For the rest of the samples aligned to more than one reference sequence, unless the percentage alignments were comparable, the best alignment is reported. Alignments with a much shorter read length than the best alignments are also omitted. For technical replicates, the best of the replicates is reported.

Sample	Consensus Genotype	Haplotype	Accession number	Filter	Aligned Read Length	I	D	M	Percentage Alignment
3	**63+*1/*1*[a]	**63*	EU530608	7680 - 9680	7739	40	53	88	97.66
5	**4.013 +*4/*1*	**4-like*	EU530605	7680 – 9680	6400	55	62	90	96.77
5	**4.013 +*4/*1*	**4N*	EU530604	7680 - 9680	7000	61	76	102	96.60
6	**4.013+*4/*4*	**4-like*	EU530605	7680 – 9680	6400	24	80	66	97.34
6	**4.013+*4/*4*	**4N*	EU530604	7680 – 9680	7000	24	80	70	97.51
6	**4.013+*4/*4*	**4.013*	PV00250 (PharmVar **4.013)*	7680 – 9680	6739	23	87	64	97.42
7	**36 + *10/*35*	**36*	PV00460 (PharmVar **36)*	7680 -12000	6739	3	13	27	99.36
7	**36 + *10/*35*	**36*	PV00705 (PharmVar **36.002*)	7680 – 9680	6737	3	11	11	99.63
7	**36 + *10/*35*	**36*	PV01364 (PharmVar **36.003*)	7680 – 9680	6739	3	13	14	99.55
7	**36 + *10/*35*	**36*	PV01720 (PharmVar **36.004*)	7680 – 9680	6737	3	11	14	99.58
8	**68+*4/*10*	**68*	EU530606	7680 -12000	4550	5	7	0	99.74
9	**4.013+*4/*1*	**4-like*	EU530605	7680 – 9680	6400	2	14	12	99.56
9	**4.013+*4/*1*	**4N*	EU530604	7680 – 9680	7000	2	14	16	99.54
9	**4.013+*4/*1*	**4.013*	PV00250 (PharmVar **4.013)*	7680 – 9680	2191	236	40	37	81.15
10	**4.013+*4/*1*	**4-like*	EU530605	7680 – 9680	6400	2	5	12	99.70
10	**4.013+*4/*1*	**4N*	EU530604	7680 – 9680	7000	2	5	16	99.67
10	**4.013+*4/*1*	**4.013*	PV00250 (PharmVar **4.013)*	7680 – 9680	6739	2	13	10	99.63

11 (NA18545)	**5/*36x2+*10x 2*	**36*	PV00460 (PharmVar **36)*	7680 – 12000	6739	3	17	23	99.36
11 (NA18545)	**5/*36x2+*10x 2*	**36*	PV00222 (PharmVar *36.001*)	7680 – 12000	6737	3	17	8	99.58
11 (NA18545)	**5/*36x2+*10x 2*	**36*	PV00705 (PharmVar *36.002*)	7680 – 9680	6737	3	15	7	99.63
11 (NA18545)	**5/*36x2+*10x 2*	**36*	PV00705 (PharmVar *36.003*)	7680 – 9680	6737	3	17	10	99.55
11 (NA18545)	**5/*36x2+*10x 2*	**36*	PV00705 (PharmVar *36.004*)	7680 – 9680	6737	3	15	10	99.58
12	**4.013+*4/*35*	**4-like*	EU530605	7680 – 9680	6400	64	103	70	96.30
12	**4.013+*4/*35*	**4N*	EU530604	7680 – 9680	6996	70	117	85	96.11
12	**4.013+*4/*35*	**4.013*	PV00250 (PharmVar *4.013)*	7680 – 9680	6726	71	123	68	96.10
14	**4.013+*4/*1*	**4-like*	EU530605	7680 – 9680	3087	7	1	2	99.68
14	**4.013+*4/*1*	**4N*	EU530604	7680 – 9680	3087	7	1	3	99.64
14	**4.013+*4/*1*	**4.013*	PV00250 (PharmVar *4.013)*	7680 – 9680	3187	7	1	2	99.69
15	**4.013 +*4/*4.002*	**4-like*	EU530605	7680 – 9680	6400	3	9	14	99.59
15	**4.013 +*4/*4.002*	**4N*	EU530604	7680 – 9680	7000	3	9	19	99.56
15	**4.013 +*4/*4.002*	**4.013*	PV00250 (PharmVar *4.013)*	7680 – 9680	6739	2	16	13	99.54
16	**4.013 +*4/*4*	**4-like*	EU530605	7680 – 9680	6037	371	166	224	87.15
16	**4.013 +*4/*4*	**4N*	EU530604	7680 – 9680	6633	408	194	262	86.97
16	**4.013 +*4/*4*	**4.013*	PV00250 (PharmVar *4.013)*	7680 – 9680	247	3	0	35	84.62
18	**4.013+*4/*2*	**4-like*	EU530605	7680 – 9680	6400	2	7	12	99.67
18	**4.013+*4/*2*	**4N*	EU530604	7680 – 9680	7000	3	5	16	99.66
18	**4.013+*4/*2*	**4.013*	PV00250 (PharmVar *4.013)*	7680 – 9680	6739	2	12	10	99.64

[a]Consensus deduced from a combination of AmpliChip CYP450 and TaqMan CNV data.

Table 2. Alignment of G amplicons to reference sequences. For samples aligned to more than one reference sequence, unless the percentage alignments were close, the best alignment is reported. Alignments with a much shorter read length than the best alignments are also omitted.

Sample	Consensus Genotype	Haplotype	Accession number	Filter	Read Length	I	D	M	Percent Alignment
22	**13/*4.013*	**13F*	EU093102	4000 – 6000	5002	1	1	1	99.94
23	**13/*1*	**13F*	EU093102	4000 – 6000	5002	153	147	122	91.56
24	**13/*1*	**13F*	EU093102	4000 – 6000	5002	15	0	3	99.64
25	**13+*2/*1*	**13A2*	GQ162807	4000 – 6000	5039	27	68	9	97.94
28	**13+*10/*36*	**13A2*	GQ162807	4000 – 6000	5039	0	1	1	99.96
30	**13/*4.013*	**13F*	EU093102	4000 – 6000	5002	2	1	0	99.94
32	**13+*2/*1*	**13A2*	GQ162807	4000 – 6000	5039	1	9	2	99.76
33	**13+*2/*1*	**13A2*	GQ162807	4000 – 6000	5039	6	1	0	99.86
37 (NA19785)	**1/*13+*2*	**13A2*	GQ162807	4000 – 6000	5039	15	27	17	98.83

Note: samples 22 and 30 are technical replicates from the same participant.

Table 3. Alignment of H amplicons to reference sequences. The best three alignments per sample are reported.

Sample	Genotype	Haplotype	Accession number	Filter	Read Length	I	D	M	Percent Alignment
39	**1/*13+*2*	**13A1*	EU098008	4000 – 6000	5026	12	27	57	98.09
39	**1/*13+*2*	**13A2*	GQ162807	4000 – 6000	5022	15	27	55	98.07
39	**1/*13+*2*	**13B*	HM641839.1	4000 – 6000	5025	12	27	46	98.31
4	**13+*4/*5*	**13C*	HM641840	4000 – 6000	5019	9	35	105	97.03
4	**13+*4/*5*	**13D*	GQ162808	4000 – 6000	5008	12	27	96	97.30
4	**13+*4/*5*	**13E*	EU098009.1	4000 – 6000	5021	7	34	98	97.23